CHIN. PHYS. LETT. Vol. 37, No. 6 (2020) 067101 **Express Letter**

Fermionic Analogue of High Temperature Hawking Radiation in Black Phosphorus *

Hang Liu(刘行)[1,5], Jia-Tao Sun(孙家涛)[1,2,5**], Chenchen Song(宋晨晨)[1,5], Huaqing Huang(黄华卿)[3], Feng Liu(刘锋)[3,4**], Sheng Meng(孟胜)[1,4,5**]

[1]*Beijing National Laboratory for Condensed Matter Physics and Institute of Physics, Chinese Academy of Sciences, Beijing 100190, China*

[2]*School of Information and Electronics, Beijing Institute of Technology, Beijing 100081, China*

[3]*Department of Materials Science and Engineering, University of Utah, Salt Lake City, Utah 84112, USA*

[4]*Collaborative Innovation Center of Quantum Matter, Beijing 100084, China*

[5]*University of Chinese Academy of Sciences, Beijing 100049, China*

(Received 18 May 2020)

Time-periodic laser driving can create nonequilibrium states not accessible in equilibrium, opening new regimes in materials engineering and topological phase transitions. We report that black phosphorus (BP) exhibits spatially nonuniform topological Floquet–Dirac states under laser illumination, mimicking the "gravity" felt by fermionic quasiparticles in the same way as that for a Schwarzschild black hole (SBH). Quantum tunneling of electrons from a type-Ⅱ Dirac cone (inside BH) to a type-I Dirac cone (outside BH) emits an SBH-like Planck radiation spectrum. The Hawking temperature $T_{\rm H}$ obtained for a fermionic analog of BH in the bilayer BP is approximately 3 K, which is several orders of magnitude higher than that in previous works. Our work sheds light on increasing $T_{\rm H}$ from the perspective of engineering 2D materials by time-periodic light illumination. The predicted SBH-like Hawking radiation, accessible in BP thin films, provides clues to probe analogous astrophysical phenomena in solids.

PACS: 71.20.−b, 78.47.−p DOI: 10.1088/0256-307X/37/6/067101

Emerging as new states of matters, topologically nontrivial phases including topological insulators and Weyl semimetals have attracted tremendous attentions in last decades.[1−17] Plenty of previous works focus on the four/two fold degenerate Dirac/Weyl points in electronic band structures.[14−22] Since Dirac cones exhibit a similar shape to light cones in the general theory of relativity, it was proposed that the gravitational black hole (BH) as a curved spacetime with an overtilted light cone has fermionic analogues in solids. To be specific, the Dirac/Weyl fermions in topological materials, with different cone shapes of type-I, type-Ⅱ and type-Ⅲ, have been proposed as platforms to most probably realize artificial BHs.[17,23−27] The motion of fermions in type-I and type-Ⅱ regions behaves like that of particles outside and inside of an artificial BH, which are separated by the type-Ⅲ region, namely, the event horizon (lower panel of Fig. 1).

Quantum fluctuation enables Hawking radiation of particles generated at the event horizon of a gravitational BH, to propagate out of and into the BH for particles and antiparticles, respectively (upper panel of Fig. 1).[28−30] The intensity of this quantum radiation is quantified by Hawking temperature ($T_{\rm H} = \kappa/2\pi$ with the gravity κ at the event horizon), which is however extremely low, $\sim 10^{-8}$ K for a BH with one solar mass.[28] This prohibitive weak intensity presents a significant challenge to directly detect Hawking radiation experimentally. On the other hand, artificial analogs including sonic BHs[31,32] in Bose–Einstein condensates,[33−36] ion rings,[37] and Fermi-degenerate liquids[38] have been proposed. Unfortunately, $T_{\rm H}$ for most artificial BHs is still very low, e.g., $\sim 10^{-9}$ K in Bose–Einstein condensates.[34] Moreover, the observation of some optical BH analogs remains controversial.[39−48] Therefore, new BH analogs inherent with quantum effects and a much higher $T_{\rm H}$ are highly desirable.

Thanks to the fact that electrostatic interactions in solids are orders of magnitude stronger than gravitational forces, an unprecedented high $T_{\rm H}$ of an artificial BH in solids can be expected.[49−51] However, two requirements for the fermionic analogue of Hawking radiation in an artificial BH are necessary: (i) a spatial distribution of band structure to produce a "steep" analogous gravity field, and (ii) a working mechanism to introduce fermionic Hawking radiation. In this work, we theoretically propose that the fermionic analogue of BH with high $T_{\rm H}$ can exist in two-dimensional (2D) BP thin films under laser illumination, which is designed to be experimentally accessible. Combining first-principles and quantum tunneling calculations, a spatially inhomogeneous system with successively distributed type-Ⅱ, -Ⅲ and -I Dirac fermions is demon-

*Supported by the National Key Research and Development Program of China (Grant Nos. 2016YFA0300902 and 2016YFA0202300), the National Basic Research Program of China (Grant No. 2015CB921001), the National Natural Science Foundation of China (Grant Nos. 11774396, 91850120 and 11974045), and the Strategic Priority Research Program (B) of CAS (Grant Nos. XDB30000000 and XDB330301). H. H. and F. L. were supported by U.S. DOE-BES (Grant No. DE-FG02-04ER46148).

**Corresponding author. Email: jtsun@iphy.ac.cn; fliu@eng.utah.edu; smeng@iphy.ac.cn

© 2020 Chinese Physical Society and IOP Publishing Ltd

strated, which acts like a Schwarzschild BH (SBH) metric to induce the electron emission from type-Ⅱ to type-I region. An effective gravity field corresponding to a strikingly high temperature $T_{\rm H} \sim 3\,{\rm K}$ is achieved, whose observation is accessible in contemporary laboratories.

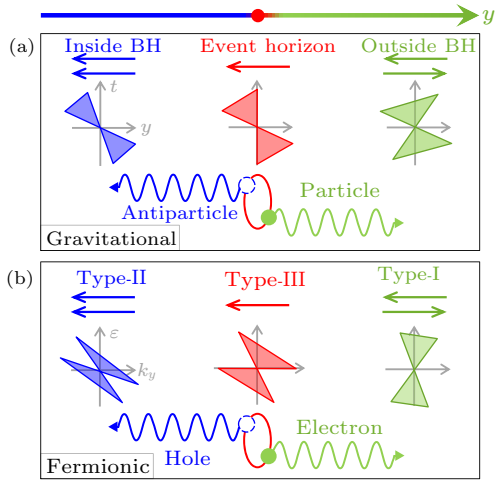

Fig. 1. Schematic illustration of gravitational Hawking radiation and fermionic analog. Upper panel: Light cones in real space indicate that particles cannot escape from gravitational BH classically (arrowed straight line), but particles and antiparticles can emit from event horizon due to quantum fluctuation (arrowed wavy line). Lower panel: Dirac cones in momentum space show that electrons cannot escape from the type-Ⅱ region (arrowed straight line) of the artificial BH in crystals, quantum tunneling enables emission of electrons and holes from the event horizon (type-Ⅲ region) to type-I and -Ⅱ regions respectively (arrowed wavy line).

Dirac fermions are classified into different types, and successive transitions between them in 2D can be described by the Hamiltonian

$$H(\boldsymbol{k}) = c_x k_x \sigma_x + c_y k_y \sigma_y + v k_y \sigma_0, \qquad (1)$$

with

$$\sigma_x = \begin{pmatrix} 0 & 1 \\ 1 & 0 \end{pmatrix}, \quad \sigma_y = \begin{pmatrix} 1 & 0 \\ 0 & -1 \end{pmatrix},$$

where σ_0 is the identity matrix. Dispersions in k_y direction are $\varepsilon_1 = (v + c_y)k_y$ and $\varepsilon_2 = (v - c_y)k_y$, whose crossing forms Dirac cone with Fermi velocities $v_{\rm F1} = v + c_y$ and $v_{\rm F2} = v - c_y$, respectively. The nodal point of the cone is known as Dirac point, whose energy is marked as $\varepsilon_{\rm D}$; $v_{\rm F1}$ and $v_{\rm F2}$ can be tuned by changing v and c_y, leading to three types of cones with distinct band dispersions and Fermi surfaces. For an upright type-I Dirac cone, $|c_y| \gg |v|$, $v_{\rm F1} = -v_{\rm F2}$. When the upright cone tilts, $|c_y|$ and $|v|$ decrease, and we elaborate here on a clockwise tilt having $c_y > 0$ and $v < 0$ [see Fig. 2(a)]. The cone remains as type-I when c_y decreases from $+\infty$ to $-v$ ($c_y > -v$). At the critical point ($c_y = -v$), the cone has a flat band of $\varepsilon_1 (v_{\rm F1} = 0,\ v_{\rm F2} < 0)$, which is dubbed type-Ⅲ with a line-like Fermi surface.[25,26] Beyond the critical point, an overtilted cone is named as type-Ⅱ having $c_y < -v$, whose two Fermi velocities have the same sign ($v_{\rm F1}$, $v_{\rm F2} < 0$) and Fermi surface encompasses both electron and hole pockets.

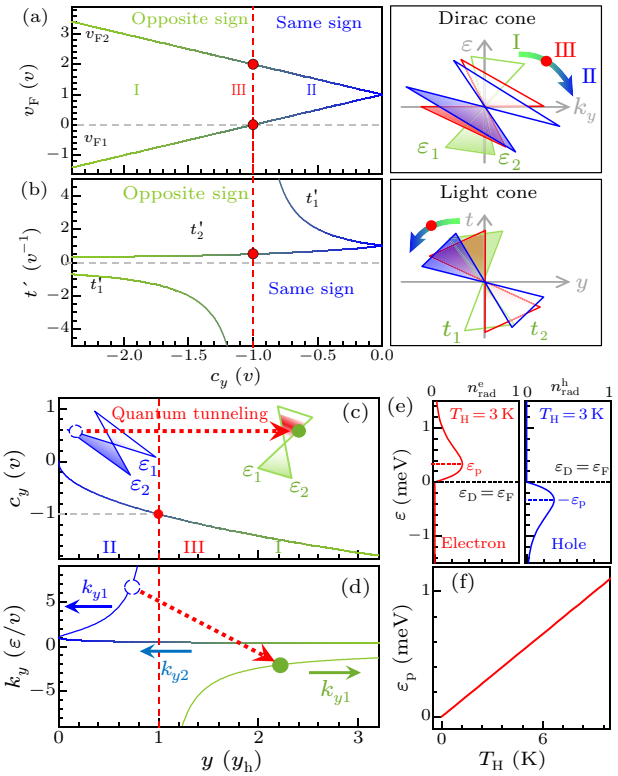

Fig. 2. Schematic illustration of fermionic analogue of a BH and consequent Hawking radiation. (a) Fermi velocity $v_{\rm F}$ of Dirac cone varies with c_y, resulting in the transition from type-I (green), type-Ⅲ (red) to type-Ⅱ (blue) Dirac cone successively. (b) Three types of artificial light cone (green, red, and blue) formed via counterclockwise rotation, corresponding to type-I, -Ⅲ, and -Ⅱ Dirac fermions respectively. (c) The distribution of c_y of type-I, -Ⅲ, and -Ⅱ Dirac fermions appears successively along $+y$ direction, producing the same "gravity field" felt by electrons as that of particles in an SBH. (d) Kinematic equation shows a high potential barrier at $y_{\rm h}$ to prevent electrons from escaping from type-Ⅱ to type-I region, but this process takes place by quantum tunneling indicated by the arrowed red dashed line in (c) and (d). (e) The spectrum of electrons (left) and holes (right) produced by Hawking radiation with $T_{\rm H} = 3\,{\rm K}$. (f) The relation between the peak position $\varepsilon_{\rm p}$ in (e) and $T_{\rm H}$.

We design a solid-state system to realize a fermionic analogue of BH. By applying a gate with the vertical electric field $E_{\rm ext}$ or compressive strain δ along armchair (x) direction, the direct band gap of 2D BP thin film decreases,[26,52–59] leading to an inversion $\Delta\varepsilon$ of valence (ε_1) and conduction (ε_2) bands. Symmetry-protected type-I Dirac cone emerges, which was confirmed by angle-resolved photoemission spectroscopy (ARPES).[55,56] For a bilayer BP, this Dirac state is shown in Fig. 3, where $\Delta\varepsilon = 14\,{\rm meV}$ at Γ point is induced by $E_{\rm ext} = 0.17\,{\rm V/Å}$ or $\delta = 7.6\%$ (for details see Fig. S1 in the Supplemental Materials, in also include some results reported in Refs.[60–66]). This is

not limited to the bilayer BP shown as an example in this work: for thicker BP films, the required strength for the external field can be even weaker.

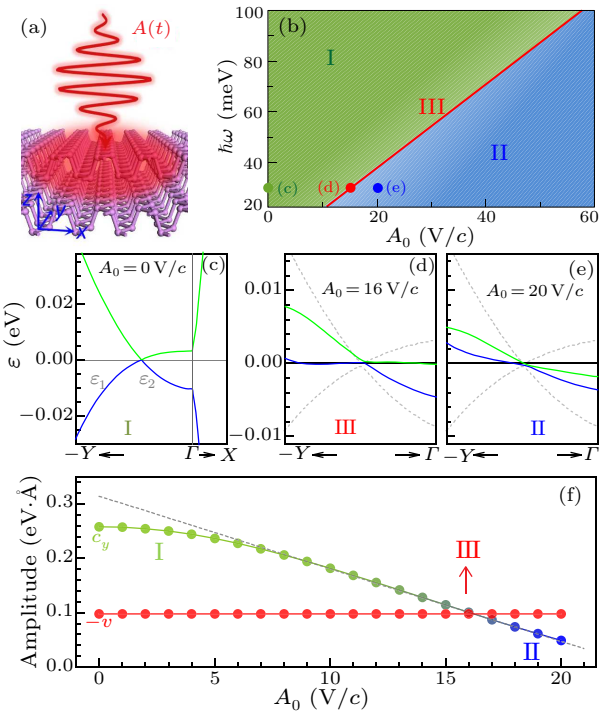

Fig. 3. First-principles calculated photoinduced type-I, -Ⅱ and -Ⅲ Dirac fermions in bilayer BP. (a) Laser field $A(t) = A_0(\sin(\omega t), 0, 0)$ is polarized along armchair (x) direction. (b) Dirac states induced by laser with different amplitude A_0 and frequency ω. (c) Band structure of bilayer BP under vertical static electric field of 0.17 V/Å. Floquet–Bloch band structure of bilayer BP driven by laser with $A_0 = 16\,\mathrm{V}/c$ (d) and $A_0 = 20\,\mathrm{V}/c$ (e), and photon energy $\hbar\omega = 0.03$ eV. (f) With increasing laser intensity, type-I Dirac fermion is transitioned to be type-Ⅲ, and -Ⅱ successively. The gray dashed line shows linear fitting of c_y vs A_0.

To form the three types of Dirac states by laser-driving, we study coherent interactions between the bilayer BP and a linearly polarized laser (LPL) with a time-dependent vector potential $\boldsymbol{A}(t) = A_0\,\sin(\omega t,\ 0,\ 0)$ [Fig. 3(a)]. The photon energy of the time-periodic and space-homogeneous LPL is chosen as $\hbar\omega = 0.03$ eV, which is larger than $\Delta\varepsilon = 14$ meV to avoid crossing nearby Dirac point between the original ($n = 0$) and photon-dressed ($n \neq 0$) bands.

Next we transform the Dirac fermions in crystals to the particles in gravity field. In Einstein's notation, Eq. (1) can be rewritten as $H(\boldsymbol{k}) = e^i_j\sigma^j k_i + e^i_0\sigma^0 k_i$ with $i, j = 1, 2$ (or x, y) and the matrix e^i_j and vector e^i_0 are equivalent to components of a tetrad field e^μ_α ($\alpha, \mu = 0, 1, 2$ in 2+1 dimensions) in general relativity. Then, an effective relativistic covariant metric $g_{\mu\nu} = (\eta^{\alpha\beta}e^\mu_\alpha e^\nu_\beta)^{-1}$ with $\eta^{\alpha\beta} = \mathrm{diag}(-1, 1, 1)$ governs Dirac fermions. The corresponding line element ($ds^2 = g_{\mu\nu}dx^\mu dx^\nu$) is

$$ds^2 = -\Big(1 - \frac{v^2}{c_y^2}\Big)dt^2 + \frac{1}{c_x^2}dx^2 + \frac{1}{c_y^2}dy^2 - \frac{2v}{c_y^2}dtdy, \quad (2)$$

which shows the behavior of Dirac quasiparticles in an effective (2+1)-dimensional (t, x, y) spacetime. For $v = 0$, $ds^2 = -c_y^2dt^2 + dy^2$ in (t, y) spacetime, representing a flat spacetime where electronic wave propagates at the velocity of c_y along $\pm y$ directions. Hence, c_y corresponds to light velocity (c) in the gravitational spacetime, so that Dirac wave propagating in a crystal field is formally equivalent to light propagating in a gravity field. In contrast to a constant c, however, the "light velocity" (c_y) in a crystal can be changed by interactions.

Effective spacetime for a given type of Dirac fermion can be designed by the relative magnitude of c_y and v. The Dirac cone manifests in its "spacetime" as an artificial light cone ($ds^2 = 0$) with $t_1 = \frac{y}{v+c_y}$ and $t_2 = \frac{y}{v-c_y}$, as shown in Fig. 2(b). For type-I, $t_1' = 1/(v + c_y) > 0$ and $t_2' = 1/(v - c_y) < 0$ having the opposite sign, quasiparticles propagate along both $+y$ and $-y$ directions. For type-Ⅲ, $t_1 \to \infty$, one branch of quasiparticles stays at a fixed location (the event horizon) permanently while the other propagates along $-y$ direction ($t_2' < 0$). For type-Ⅱ, both t_1' and t_2' are negative, all quasiparticles propagate along $-y$ direction resembling the unidirectional behavior of particles inside an SBH.

In the bilayer BP, when the LPL is applied, the type-I Dirac cone tilts due to the hybridization between $n = 0$ and $n \neq 0$ bands. At the critical laser amplitude $A_0 = 16\,\mathrm{V}/c$ (corresponding to 0.24 mV/Å or 7.65×10^5 W/cm^2, where c is the speed of light in vacuum), ε_1 band along Γ–Y path becomes flat, forming type-Ⅲ Dirac cone [Fig. 3(d)]. As the laser amplitude increases to $A_0 = 20\,\mathrm{V}/c$, the Dirac cone tilts further to become type-Ⅱ [Fig. 3(e)]. Then the slope of ε_1 and ε_2 dispersions has the same sign, and the states of the ε_1 band above Fermi level ($\varepsilon_1 > 0$ eV) becomes occupied. Consequently, type-I, Ⅱ and -Ⅲ Dirac fermions are created in a single material of 2D BP by a varying laser intensity. In addition, laser frequency also plays a crucial role in determining the type of cones, which is shown in the phase diagram of Fig. 3(b). To study structure stability of the laser-driven bilayer BP, we performed first-principles simulations based on time-dependent density functional theory.[65,66] Importantly, we found that no layer deformation or bond breaking taking place in bilayer BP thin films under a laser illumination with electric field amplitude 0.3 mV/Å used here (see Fig. S3 in the Supplementary Materials for details).

To mimic the spacetime geometry of Eq. (2), we map the photoinduced Dirac states from *ab initio* calculations to model parameters in Eq. (1). As shown in Fig. 3(f), the parameter $v = -0.1$ eV·Å is constant, while c_y decreases gradually with increasing A_0, showing the transition from type-I ($c_y > -v$) to type-Ⅱ ($c_y < -v$). In the regime of strong (weak) laser intensity, c_y and A_0 exhibit a linear (nonlinear) relation,

which is a typical characteristics of optical Stark effect (see Fig. S4 in the Supplementary Materials for details). Neglecting the small nonlinearity, one can fit c_y and A_0 as

$$c_y\,[\text{eV}\cdot\text{Å}] = 0.314 - 0.013A_0\,[\text{V}/c], \tag{3}$$

which is the base to explore Hawking radiation in the laser-driven bilayer BP thin film.

To produce a desired gravity field for Dirac fermions, an appropriate spatial distribution of effective geometry is designed. Matching the effective and Schwarzschild metrics,[67] the effective potential energy of quasiparticles is $\Phi(y) = -\frac{1}{2}\frac{v^2(y)}{c_y^2(y)}$. $\Phi(y)$ is inversely proportional to the distance: $\Phi(y) = -\frac{1}{2}\frac{y_\text{h}}{y}$, where y_h is the location of event horizon. Consequently, the effective light velocity c_y distributes along the y direction as

$$c_y(y) = -v\sqrt{\frac{y}{y_\text{h}}}. \tag{4}$$

This guarantees that type-Ⅱ fermions are inside the BH ($0 < y < y_\text{h}$), type-Ⅲ at the event horizon ($y = y_\text{h}$) and type-I outside the BH ($y > y_\text{h}$) [Fig. 2(c)]. The motion of quasiparticles is described by kinematic equations of

$$k_{y1} = \frac{\varepsilon_1}{v(1-\sqrt{y/y_\text{h}})},\quad k_{y2} = \frac{\varepsilon_2}{v(1+\sqrt{y/y_\text{h}})}.$$

As shown in Fig. 2(d), k_{y1} and k_{y2} represent two ingoing waves inside the BH, and one ingoing and one outgoing wave outside the BH. At the event horizon, there is such a high potential barrier that quasiparticles occupying on the ε_1 band are impossible to go through classically, but can tunnel through via quantum fluctuation to produce Hawking radiation.

Using quantum tunneling method,[50,68] we analyze the analogous Hawking radiation at the effective BH event horizon with the curved geometry of Eq. (4). As illustrated in Fig. 2(c), the ε_1 states above the Dirac point ($\varepsilon_1 > \varepsilon_\text{D}$) are occupied inside the BH, but empty outside. This leads to emission of the excited electrons from inside to outside the BH. Adopting Wentzel–Kramers–Brillouin approximation, the tunneling probability is $P = 1/[1 + \exp(2S)]$ with a classical action $S = \Im\int k_y(y)dy$. Assuming $k_y \approx \varepsilon[\frac{dc_y}{dy}|_{y_\text{h}}\cdot(y-y_\text{h})]^{-1}$ for the k_{y1} branch around the event horizon, P produces a spectrum with the energy intensity $I(\varepsilon) = n^\text{e}_\text{rad}(\varepsilon)\cdot\varepsilon$. The number of radiated electrons follows

$$n^\text{e}_\text{rad}(\varepsilon) \propto \frac{\varepsilon}{\exp(\frac{\varepsilon}{k_\text{B}T_\text{H}})+1}, \tag{5}$$

where k_B is the Boltzmann constant, and T_H is the Hawking temperature,

$$T_\text{H} = \frac{1}{2\pi k_\text{B}}\left|\frac{d}{dy}(c_y - v)\right|_{y_\text{h}}.$$

Substituting c_y in Eq. (3) with Eq. (4), the amplitude of space-inhomogeneous laser field is $A_0(y)\,[\text{V}/c] = -8.154\sqrt{y\,[\text{Å}]/y_\text{h}\,[\text{Å}]} + 24.1538$, leading to $T_\text{H} = \frac{-v}{4\pi k_\text{B}y_\text{h}}$. Similar to $T_\text{H} \propto \frac{c}{r_\text{h}}$ for a gravitational BH, the T_H of the proposed artificial BH is inversely proportional to the size (y_h) of a BH. In the cases of gravitational BH, r_h is determined by the mass of BH, $r_\text{h} = 2GM$, with G being the gravitational constant and M the mass of BH. Here one can intentionally control the focus area of light with a suitable intensity to achieve a small r_h (i.e., a small analogous mass) and thus a high T_H. To achieve $T_\text{H} = 3\,\text{K}$, the BH size is set at $y_\text{h} = 30.2\,\text{Å}$, which requires the laser field to decrease from 0.37 to 0 mV/Å in a range of 260 Å along the zigzag (y) direction of BP [Fig. 4(a)]. This gradient of laser intensity can be readily realized in experiments.[69–71]

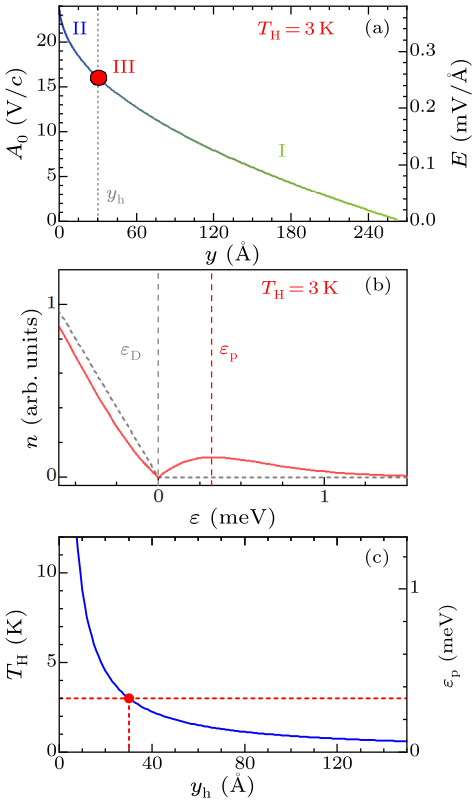

Fig. 4. The theoretically designed Hawking radiation in a bilayer BP thin film. (a) Required laser intensity distribution along zigzag (y) direction to realize an SBH with $T_\text{H} = 3\,\text{K}$. (b) The electron distribution $n(\varepsilon)$ at $y > y_\text{h}$ after Hawking radiation with $T_\text{H} = 3\,\text{K}$. The $n_0(\varepsilon)$ before Hawking radiation is shown by the gray-dashed line. (c) The calculated dependence of T_H on the location of event horizon. The red dot corresponds to $T_\text{H} = 3\,\text{K}$ and $\varepsilon_\text{p} = 0.3\,\text{meV}$.

The radiated Hawking spectrum $I(\varepsilon)$ can be measured from the local electron distribution $n(\varepsilon)$ in the region $y > y_\text{h}$, using for instance scanning tunneling spectroscopy (STS) or ARPES. The energy spectrum $I(\varepsilon) = n^\text{e}_\text{rad}(\varepsilon)\cdot\varepsilon$ of radiated massless Dirac electrons conforms to the thermal radiation of massless Dirac

particles from a 2D gravitational BH (see the Supplementary Materials). The "radiated" electrons and holes created by quantum fluctuation are entangled (lower panel in Fig. 1). It will also be very interesting to study the correlation effects between a Hawking pair (electron-hole pair) using our proposed fermionic analog of BH, such as by detecting and analyzing the distributions of both electrons (in the type-Ⅱ region) and holes (type-I region) simultaneously resulted from quantum tunneling.

As shown in Fig. 2(e), the energy of $\varepsilon = 0$ is set as the Fermi level ($\varepsilon_{\rm F}$), at which Dirac point and chemical potential locate ($\varepsilon_{\rm D} = \varepsilon_{\rm F} = 0$). The spectrum $n^{\rm e}_{\rm rad}(\varepsilon)$ with $\varepsilon > \varepsilon_{\rm D}$ has a peak at $\varepsilon_{\rm p} = 0.3\,{\rm meV}$ for $T_{\rm H} = 3\,{\rm K}$, which is distinct from the Fermi–Dirac distribution; and $n^{h}_{\rm rad}(\varepsilon)$ for radiated holes below $\varepsilon_{\rm D}$ due to quantum tunneling is similar. The Hawking spectrum (in 2D) derived here is the same as that of massless fermions emitted from a 2D BH, providing a key signature for Hawking radiation. $T_{\rm H}$ can be tuned by controlling the effective gravity field to facilitate the experimental detection of $n^{\rm e}_{\rm rad}(\varepsilon)$ and $n^{h}_{\rm rad}(\varepsilon)$. The relation between $\varepsilon_{\rm p}$ and $T_{\rm H}$ follows

$$\frac{\varepsilon_{\rm p}}{k_{\rm B}T_{\rm H}} = 1 + \exp\left(-\frac{\varepsilon_{\rm p}}{k_{\rm B}T_{\rm H}}\right),$$

leading to a linear dependence $\varepsilon_{\rm p} = 1.28 k_{\rm B} T_{\rm H}$ [Fig. 2(f)]. An unprecedentedly high $T_{\rm H}$ is achieved because interactions in crystals are orders of magnitude stronger than those in gravity field and Bose–Einstein condensate.

The well-designed setup to probe fermionic analogue of Hawking radiation is readily accessible in experiment. Firstly, the high-quality crystal of 2D BP (as a familiar material) is routinely prepared by traditional experimental approaches.[55,56] Secondly, the required laser field with maximum amplitude of $0.37\,{\rm mV/Å}$, photon energy of $0.03\,{\rm eV}$, and space gradient of $1.4\,{\rm \mu V/Å}^{\,2}$ is currently attainable in experiment.[69–71] Thirdly, the Planck radiation spectrum can be measured by contemporary scanning tunneling spectroscopy[72] or angle-resolved photoemission spectroscopy.[73] The radiation could be confirmed by measuring electron distribution $n(\varepsilon) = n_0(\varepsilon) + n^{\rm e}_{\rm rad}(\varepsilon) - n^{h}_{\rm rad}(\varepsilon)$ in the region $y > y_{\rm h}$, where $n^{\rm e}_{\rm rad}(\varepsilon)$ and $n^{h}_{\rm rad}(\varepsilon)$ are the radiated spectrum of electrons and holes in Fig. 2(e), respectively, and $n_0(\varepsilon)$ is the electron distribution before radiation. As shown in Fig. 4(b), the peak position $\varepsilon_{\rm p}$ of the distribution $n(\varepsilon)$ is calculated to be 0.3 meV above the Fermi level, readily resolvable in experiment.[72,73] Decreasing the BH size, $\varepsilon_{\rm p}$ increases in a wide range of $T_{\rm H}$ [Fig. 4(c)]. Also, we note that there are a pair of Dirac cones along $-YY$ path resembling black and white holes respectively, but their coexistence does not influence the Hawking radiation (see details in Fig. S5).

In conclusion, type-I, -Ⅱ and -Ⅲ Dirac fermions are predicted to form in 2D BP thin film under LPL, resulting in a fermionic analogue of BH Hawking radiation. Hawking temperature is theoretically estimated to reach 3 K, with the emitted electrons exhibiting a spectrum peaked at 0.3 meV above the Fermi level, which is experimentally observable.[72,73] Despite being intrinsically a nonequilibrium phenomenon, the quantum theory analysis and first-principles confirmation are well applicable since the system would reach a quasi-stationary steady state in a real setup. Our finding opens a path to engineering the table-top fermionic condensed-matter platform for simulating exotic phenomena in astrophysics and general relativity.

References

[1] Klitzing K V, Dorda G and Pepper M 1980 *Phys. Rev. Lett.* **45** 494
[2] Thouless D J, Kohmoto M, Nightingale M P and den Nijs M 1982 *Phys. Rev. Lett.* **49** 405
[3] Tsui D C, Stormer H L and Gossard A C 1982 *Phys. Rev. Lett.* **48** 1559
[4] Laughlin R B 1983 *Phys. Rev. Lett.* **50** 1395
[5] Haldane F D 1988 *Phys. Rev. Lett.* **61** 2015
[6] Yu R, Zhang W, Zhang H J, Zhang S C, Dai X and Fang Z 2010 *Science* **329** 61
[7] Chang C Z, Zhang J, Feng X, Shen J, Zhang Z, Guo M, Li K, Ou Y, Wei P, Wang L L, Ji Z Q, Feng Y, Ji S, Chen X, Jia J, Dai X, Fang Z, Zhang S C, He K, Wang Y, Lu L, Ma X C and Xue Q K 2013 *Science* **340** 167
[8] Kane C L and Mele E J 2005 *Phys. Rev. Lett.* **95** 226801
[9] Bernevig B A, Hughes T L and Zhang S C 2006 *Science* **314** 1757
[10] Koenig M, Wiedmann S, Bruene C, Roth A, Buhmann H, Molenkamp L W, Qi X L and Zhang S C 2007 *Science* **318** 766
[11] Novoselov K S, Geim A K, Morozov S V, Jiang D, Zhang Y, Dubonos S V, Grigorieva I V and Firsov A A 2004 *Science* **306** 666
[12] Zhu Z, Winkler G W, Wu Q, Li J and Soluyanov A A 2016 *Phys. Rev. X* **6** 031003
[13] Bradlyn B, Cano J, Wang Z, Vergniory M G, Felser C, Cava R J and Bernevig B A 2016 *Science* **353** aaf5037
[14] Wang Z, Sun Y, Chen X Q, Franchini C, Xu G, Weng H, Dai X and Fang Z 2012 *Phys. Rev. B* **85** 195320
[15] Wan X, Turner A M, Vishwanath A and Savrasov S Y 2011 *Phys. Rev. B* **83** 205101
[16] Weng H M, Fang C, Fang Z, Bernevig B A and Dai X 2015 *Phys. Rev. X* **5** 011029
[17] Soluyanov A A, Gresch D, Wang Z, Wu Q, Troyer M, Dai X and Bernevig B A 2015 *Nature* **527** 495
[18] Lv B Q, Weng H M, Fu B B, Wang X P, Miao H, Ma J, Richard P, Huang X C, Zhao L X, Chen G F, Fang Z, Dai X, Qian T and Ding H 2015 *Phys. Rev. X* **5** 031013
[19] Lv B Q, Xu N, Weng H M, Ma J Z, Richard P, Huang X C, Zhao L X, Chen G F, Matt C E, Bisti F, Strocov V N, Mesot J, Fang Z, Dai X, Qian T, Shi M and Ding H 2015 *Nat. Phys.* **11** 724
[20] Huang X C, Zhao L X, Long Y J, Wang P P, Chen D, Yang Z H, Liang H, Xue M Q, Weng H M, Fang Z, Dai X and Chen G F 2015 *Phys. Rev. X* **5** 031023
[21] Huang S M, Xu S Y, Belopolski I, Lee C C, Chang G Q, Wang B K, Alidoust N, Bian G, Neupane M, Zhang C L, Jia S, Bansil A, Lin H and Hasan M Z 2015 *Nat. Commun.* **6** 7373
[22] Lv B Q, Muff S, Qian T, Song Z D, Nie S M, Xu N, Richard P, Matt C E, Plumb N C, Zhao L X, Chen G F, Fang Z, Dai X, Dil J H, Mesot J, Shi M, Weng H M and Ding H 2015 *Phys. Rev. Lett.* **115** 217601

[23] Volovik G E and Zhang K 2017 *J. Low Temp. Phys.* **189** 276
[24] Guan S, Yu Z M, Liu Y, Liu G B, Dong L, Lu Y, Yao Y and Yang S A 2017 *npj Quantum Mater.* **2** 23
[25] Huang H, Jin K H and Liu F 2018 *Phys. Rev. B* **98** 121110(R)
[26] Liu H, Sun J T, Cheng C, Liu F and Meng S 2018 *Phys. Rev. Lett.* **120** 237403
[27] Weststrom A and Ojanen T 2017 *Phys. Rev. X* **7** 041026
[28] Hawking S W 1974 *Nature* **248** 30
[29] Hartle J B and Hawking S W 1976 *Phys. Rev. D* **13** 2188
[30] Bardeen J M 1981 *Phys. Rev. Lett.* **46** 382
[31] Unruh W G 1981 *Phys. Rev. Lett.* **46** 1351
[32] Unruh W G 1995 *Phys. Rev. D* **51** 2827
[33] Garay L J, Anglin J R, Cirac J I and Zoller P 2000 *Phys. Rev. Lett.* **85** 4643
[34] Lahav O, Itah A, Blumkin A, Gordon C, Rinott S, Zayats A and Steinhauer J 2010 *Phys. Rev. Lett.* **105** 240401
[35] Garay L J, Anglin J R, Cirac J I and Zoller P 2001 *Phys. Rev. A* **63** 023611
[36] Steinhauer J 2016 *Nat. Phys.* **12** 959
[37] Horstmann B, Reznik B, Fagnocchi S and Cirac J I 2010 *Phys. Rev. Lett.* **104** 250403
[38] Giovanazzi S 2005 *Phys. Rev. Lett.* **94** 061302
[39] Leonhardt U and Piwnicki P 2000 *Phys. Rev. Lett.* **84** 822
[40] Leonhardt U 2002 *Nature* **415** 406
[41] Schutzhold R and Unruh W G 2005 *Phys. Rev. Lett.* **95** 031301
[42] Philbin T G, Kuklewicz C, Robertson S, Hill S, Konig F and Leonhardt U 2008 *Science* **319** 1367
[43] Belgiorno F, Cacciatori S L, Clerici M, Gorini V, Ortenzi G, Rizzi L, Rubino E, Sala V G and Faccio D 2010 *Phys. Rev. Lett.* **105** 203901
[44] Schutzhold R and Unruh W G 2011 *Phys. Rev. Lett.* **107** 149401
[45] Elazar M, Fleurov V and Bar-Ad S 2012 *Phys. Rev. A* **86** 063821
[46] Liberati S, Prain A and Visser M 2012 *Phys. Rev. D* **85** 084014
[47] Unruh W G and Schützhold R 2003 *Phys. Rev. D* **68** 024008
[48] Unruh W G and Schützhold R 2012 *Phys. Rev. D* **86** 064006
[49] Han T, Kribs G D and McElrath B 2003 *Phys. Rev. Lett.* **90** 031601
[50] Corda C 2015 *Class. Quantum Grav.* **32** 195007
[51] Kerner R and Mann R B 2008 *Class. Quantum Grav.* **25** 095014
[52] Ling X, Wang H, Huang S X, Xia F N and Dresselhaus M S 2015 *Proc. Natl. Acad. Sci. USA* **112** 4523
[53] Rodin A S, Carvalho A and Castro Neto A H 2014 *Phys. Rev. Lett.* **112** 176801
[54] Deng B, Tran V, Xie Y, Jiang H, Li C, Guo Q, Wang X, Tian H, Koester S J, Wang H, Cha J J, Xia Q, Yang L and Xia F 2017 *Nat. Commun.* **8** 14474
[55] Kim J, Baik S S, Ryu S H, Sohn Y, Park S, Park B G, Denlinger J, Yi Y, Choi H J and Kim K S 2015 *Science* **349** 723
[56] Kim J, Baik S S, Jung S W, Sohn Y, Ryu S H, Choi H J, Yang B J and Kim K S 2017 *Phys. Rev. Lett.* **119** 226801
[57] Zhao J, Yu R, Weng H and Fang Z 2016 *Phys. Rev. B* **94** 195104
[58] Li L, Yu Y, Ye G J, Ge Q, Ou X, Wu H, Feng D, Chen X H and Zhang Y 2014 *Nat. Nanotechnol.* **9** 372
[59] Dutreix C, Stepanov E A and Katsnelson M I 2016 *Phys. Rev. B* **93** 241404
[60] Kresse G and Furthmuller J 1996 *Phys. Rev. B* **54** 11169
[61] Perdew J P, Burke K and Ernzerhof M 1996 *Phys. Rev. Lett.* **77** 3865
[62] Mostofi A A, Yates J R, Lee Y S, Souza I, Vanderbilt D and Marzari N 2008 *Comput. Phys. Commun.* **178** 685
[63] Mostofi A A, Yates J R, Pizzi G, Lee Y S, Souza I, Vanderbilt D and Marzari N 2014 *Comput. Phys. Commun.* **185** 2309
[64] Marzari N, Mostofi A A, Yates J R, Souza I and Vanderbilt D 2012 *Rev. Mod. Phys.* **84** 1419
[65] Runge E and Gross E K U 1984 *Phys. Rev. Lett.* **52** 997
[66] Meng S and Kaxiras E 2008 *J. Chem. Phys.* **129** 054110
[67] Volovik G E, *The Universe in a Helium Droplet (Oxford: Oxford University Press)*
[68] Parikh M K 2000 *Phys. Rev. Lett.* **85** 5042
[69] Roberts A, Cormode D, Reynolds C, Newhouse-Illige T, LeRoy B J and Sandhu A S 2011 *Appl. Phys. Lett.* **99** 051912
[70] Wang Y H, Steinberg H, Jarillo-Herrero P and Gedik N 2013 *Science* **342** 453
[71] Mahmood F, Chan C K, Alpichshev Z, Gardner D, Lee Y, Lee P A and Gedik N 2016 *Nat. Phys.* **12** 306
[72] Wiebe J, Wachowiak A, Meier F, Haude D, Foster T, Morgenstern M and Wiesendanger R 2004 *Rev. Sci. Instrum.* **75** 4871
[73] Liu G, Wang G, Zhu Y, Zhang H, Zhang G, Wang X, Zhou Y, Zhang W, Liu H, Zhao L, Meng J, Dong X, Chen C, Xu Z and Zhou X J 2008 *Rev. Sci. Instrum.* **79** 023105

Supplemental Material: Fermionic analogue of high temperature Hawking radiation in black phosphorus

Hang Liu (刘行)[1,5], Jia-Tao Sun (孙家涛)[1,2,5] , Chenchen Song (宋晨晨)[1,5], Huaqing Huang(黄华卿)[3], Feng Liu (刘锋)[3,4] , Sheng Meng (孟胜)[1,4,5]

[1] Beijing National Laboratory for Condensed Matter Physics and Institute of Physics, Chinese Academy of Sciences, Beijing 100190, China

[2] School of Information and Electronics, Beijing Institute of Technology, Beijing 100081, China

[3] Department of Materials Science and Engineering, University of Utah, Salt Lake City, Utah 84112, USA

[4] Collaborative Innovation Center of Quantum Matter, Beijing 100084, China

[5] University of Chinese Academy of Sciences, Beijing 100049, China

We present the Supplemental Materials for the computational methods, Hawking spectrum derivation, electronic bands in equilibrium BP, choice of laser polarization, stability of laser-driven BP, coexisting analogous black and white holes in 2D BP, which includes some results in Refs. [60-66].

A. Computational methods

First-principle calculations are performed by Vienna Ab-initio Simulation Package (VASP)[60] to obtain Bloch bands of bilayer black phosphorous (BP) in equilibrium. The projector-augmented wave (PAW) pseudopotential and Perdew-Burke-Ernzerhof (PBE) functional[61] are adopted. The energy cutoff of plane-wave basis set is set as 400 eV and the Brillouin zone is sampled by $9 \times 9 \times 1$ Gamma centered k-mesh. The atomic structures are relaxed until the force on each atom is less than 0.01 eV/Å. The convergence condition of electronic self-consistence is 10^{-6} eV. Bloch band structures are expanded in the Wannier basis, in which s, p_x, p_y and p_z orbitals of every P atom are chosen as projected orbitals. Based on Floquet theorem, laser-driven electronic structures of bilayer BP is computed[62-64]. Besides, to study the structure stability of BP, we employ the home-made time-dependent ab initio package to perform molecular dynamics simulations of BP under laser illumination within time-dependent density functional theory (TDDFT)[65,66]. The 2×2 supercell of bilayer BP with 32 atoms is adopted, with a $\boldsymbol{k}$-point mesh of $4 \times 5 \times 1$ and the mesh cutoff 200 Ry. The simulations last for > 2 ps with a time step 0.05 fs, where the photon energy is fixed at 0.03 eV.

B. Derivation of Hawking spectrum from a 2D fermionic analog of BH

For electrons above the Fermi level in the region with type-II fermions, they will be emitted to the

region with type-I fermions through the potential barrier at the event horizon of y_h. This process can be modeled by a quantum tunneling process. Around $y = y_h$, the quasimomentum of electrons can be approximated by

$$k_y \approx \frac{\varepsilon}{\left(\frac{dc_y}{dy}\right)\Big|_{y_h} \cdot (y - y_h)}, \tag{S1}$$

where c_y is the parameter in the Dirac Hamiltonian of Eq. (1) in the main text. The classical action for quasiparticles equals to the imaginary part of moment integration

$$S = \mathrm{Im}\int k_y(y)dy = \pi \frac{\varepsilon}{\left(\frac{dc_y}{dy}\right)\Big|_{y_h}}, \tag{S2}$$

which is calculated by using contour integral and residue theorem. According to Wentzel-Kramers-Brillouin approximation, the relative tunneling probability from type-II to type-I region is

$$P_{rel} = \exp\left(-\frac{2S}{\hbar}\right) = \exp\left(-\frac{\varepsilon}{k_B T_H}\right), \tag{S3}$$

where $T_H = \frac{\hbar}{2\pi k_B}\left|\frac{d}{dy}(c_{//} - v)\right|_{y_h}$. For fermions, the relative (P_{rel}) and absolute (P_{abs}) tunneling probability conforms to $P_{abs} + \frac{P_{abs}}{P_{rel}} = 1$, resulting in

$$P_{abs} = \frac{1}{\exp\left(\frac{\varepsilon}{k_B T_H}\right) + 1}. \tag{S4}$$

Similar to light, Dirac electrons in two dimensions also possess a linear dispersion $\varepsilon \propto k$, which indicates that the number of states per unit area, per unit energy for Dirac electrons inside the type-II region is proportional to ε. Thus, the number of the radiated electrons from type-II (inside BH) to type-I region (outside BH) follows

$$n^{\mathrm{e}}{}_{\mathrm{rad}}(\varepsilon) \propto \frac{\varepsilon}{\exp\left(\frac{\varepsilon}{k_B T_H}\right) + 1}, \quad \text{with } \varepsilon > 0, \tag{S5}$$

which was also shown in the Eq. (4) in the main text. Therefore, the radiation energy spectrum is

$$I(\varepsilon) = n^{\mathrm{e}}{}_{\mathrm{rad}}(\varepsilon) \cdot \varepsilon \propto \frac{\varepsilon^2}{\exp\left(\frac{\varepsilon}{k_B T_H}\right) + 1}. \tag{S6}$$

The radiated energy distribution $I(\varepsilon)$ clearly exhibits the form of radiation spectrum of massless fermions from a 2D black hole, indicating that the proposed radiation is an analog of Hawking radiation with a temperature of T_H.

TABLE S1. The formulas of black hole (Hawking) radiation.

(Quasi)particle / Radiation		Photon (Massless boson)			Massless Dirac		
		DOS	P	n	DOS	P	n
Gravitational black hole	3D	$\propto \varepsilon^2$	$\frac{1}{e^{\varepsilon/kT_H}-1}$	$\propto \varepsilon^2 \cdot \frac{1}{e^{\varepsilon/kT_H}-1}$ (Planck spectrum)	$\propto \varepsilon^2$	$\frac{1}{e^{\varepsilon/kT_H}+1}$	$\propto \varepsilon^2 \cdot \frac{1}{e^{\varepsilon/kT_H}+1}$
	2D	$\propto \varepsilon$	$\frac{1}{e^{\varepsilon/kT_H}-1}$	$\propto \varepsilon \cdot \frac{1}{e^{\varepsilon/kT_H}-1}$	$\propto \varepsilon$	$\frac{1}{e^{\varepsilon/kT_H}+1}$	$\propto \varepsilon \cdot \frac{1}{e^{\varepsilon/kT_H}+1}$
Fermionic analog	2D	—	—	—	$\propto \varepsilon$	$\frac{1}{e^{\varepsilon/kT_H}+1}$	$\propto \varepsilon \cdot \frac{1}{e^{\varepsilon/kT_H}+1}$

Note: i) DOS = density of occupied states;

ii) P = tunneling probability of a single particle;

iii) n = DOS×P is the number distribution of radiated particles, and the energy spectrum is $I = n \times \varepsilon$.

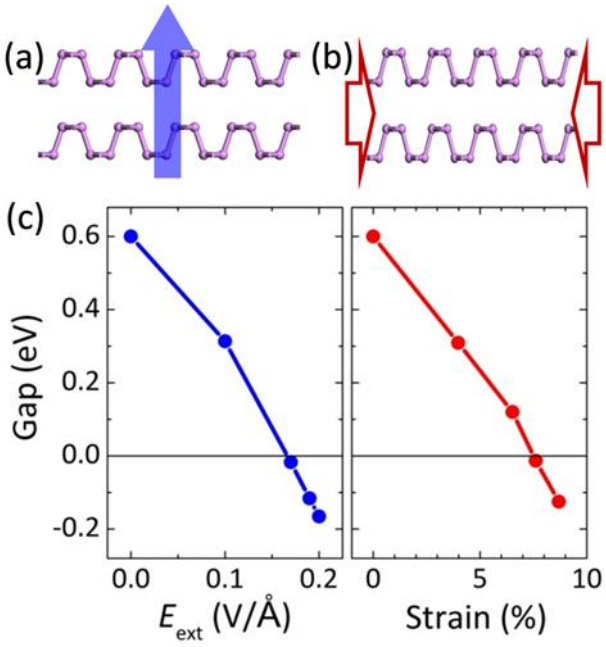

FIG. S1. Band gap variation of bilayer black phosphorous induced by a vertical electrical field [(a) and left panel in (c)], and compressive strain along armchair direction [(b) and right panel in (c)].

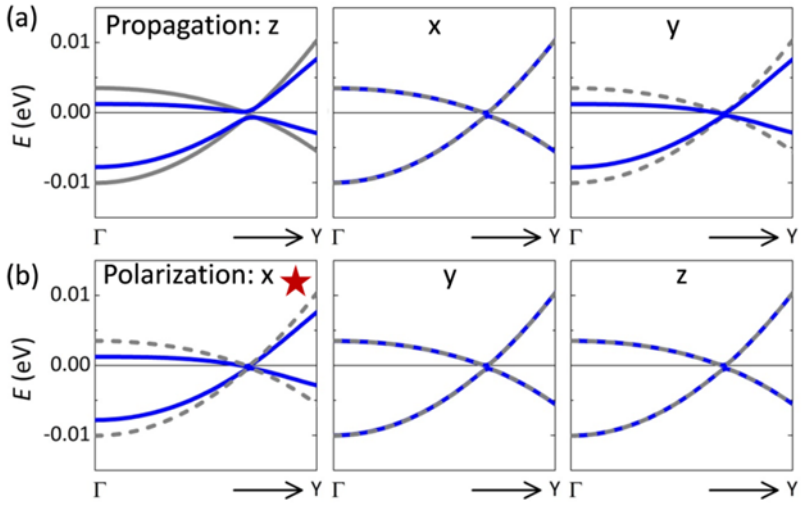

FIG. S2. Floquet-Bloch band structure (blue line) induced by laser with photon energy $\hbar\omega$ = 0.03 eV and amplitude A_0 = 10V/c. (a) Circularly polarized laser with z, x, and y propagation directions, respectively. (b) Linearly polarized laser with polarization direction of x, y, and z from left to right. Gray lines represent bands in equilibrium states.

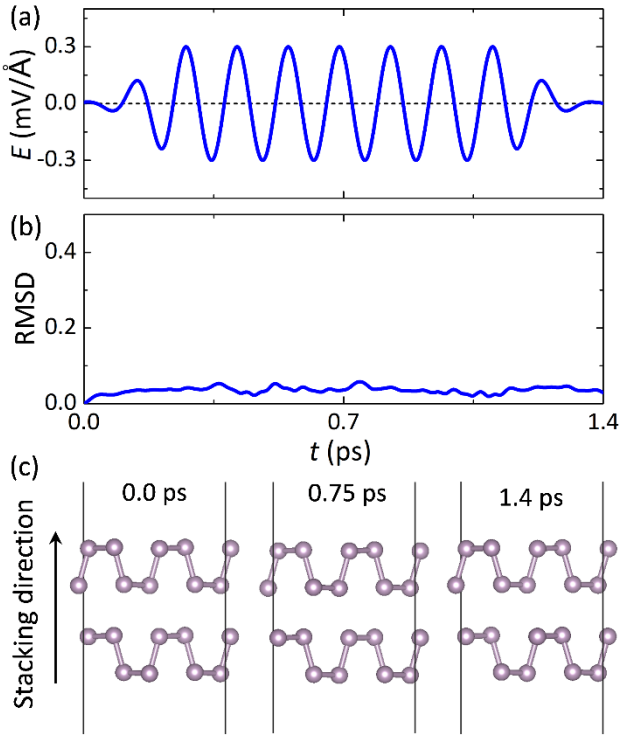

FIG. S3. Structure stability of light driven bilayer BP from TDDFT calculations. (a) Electric field of a linearly polarized laser with photon energy 0.03eV and amplitude 0.3mV/Å. The pulse envelope is chosen to be a trapezium for realizing Floquet states. (b) The evolution of root-mean-square displacement (RMSD) with time. (c) Atomic structures at t = 0, 0.75, and 1.4 ps.

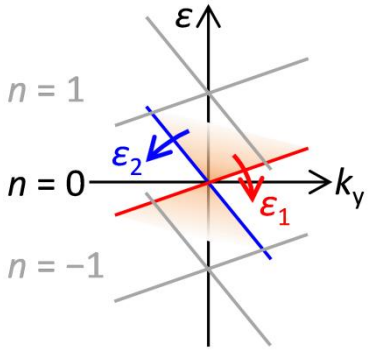

FIG. S4. Renormalized dispersions around Dirac cone due to the interactions between original and dressed bands. Under laser illumination, original bands with index $n = 0$ absorb (emit) one photon to form $n = 1$ ($n = -1$) dressed bands, whose hybridization would lead to gaps at crossings of $n = 0$ and $n = \pm 1$ bands due to optical Stark effect. Consequently, the bands of ε_1 and ε_2 would rotate around the Dirac point along clockwise and anticlockwise directions, respectively. Laser driving cannot change the value of $v = \frac{1}{2}\cdot\frac{\partial(\varepsilon_1+\varepsilon_2)}{\partial k_y}$ due to the inverse variation of ε_1 and ε_2, but the parameter of $c_y = \frac{1}{2}\cdot\frac{\partial(\varepsilon_1-\varepsilon_2)}{\partial k_y}$ can be varied significantly.

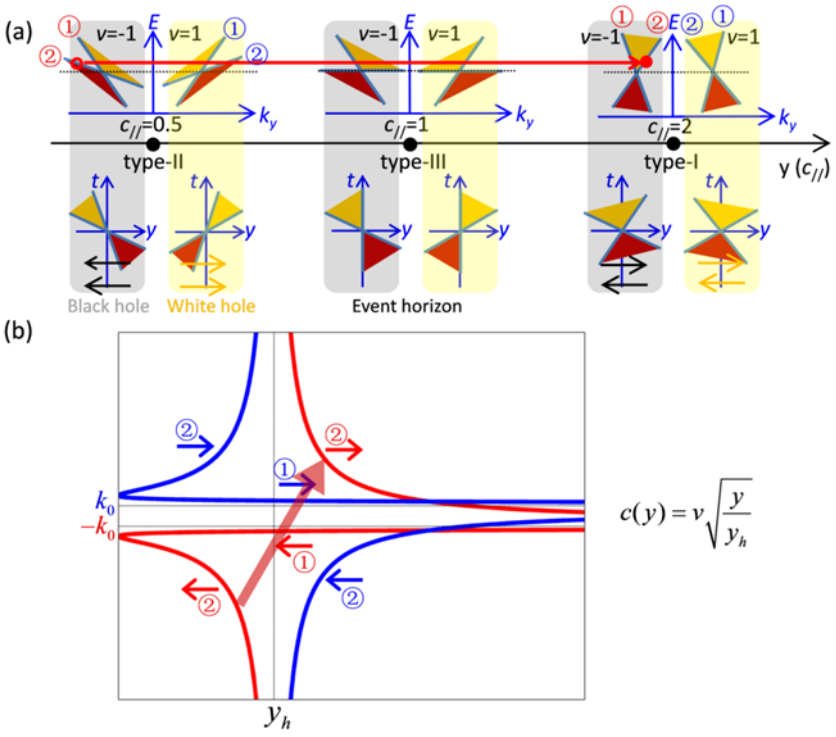

FIG. S5. Hawking radiation in a system with coexisting artificial black and white holes. (a) Electron band structure and corresponding light cones vary with space. (b) Tunneling mechanism.